Isoscalar giant resonance strength in ^{24}Mg

D. H. Youngblood, Y.-W. Lui, X. F. Chen,* and H. L. Clark

Cyclotron Institute, Texas A&M University, College Station, Texas 77843, USA

The giant resonance region from 9 MeV $< E_x <$ 60 MeV in ^{24}Mg has been studied with inelastic scattering of 240-MeV α particles at small angles, including $0°$. Isoscalar $E0$, $E1$, $E2$, and $E3$ strength was identified from 9 MeV $< E_x <$ 40 MeV and the effects of differing continua studied.

The properties of the isoscalar giant resonances in nuclei are important because of what they tell us of the bulk nuclear properties. The isoscalar giant monopole resonance (GMR) is of particular importance because its energy can be directly related to the nuclear compressibility, and from this, the compressibility of nuclear matter (K_{NM}) can be obtained. Initial studies of the GMR in ^{24}Mg with 120-MeV α [1] and 156-MeV ^{6}Li [2] inelastic scattering identified monopole strength over a limited energy range ($10 < E_x < 23$ MeV). In 1999, using inelastic scattering of 240-MeV α particles [3], $E0$ strength was identified extending up to $E_x = 40$ MeV. In that experiment, isoscalar $E0$ [72% energy-weighted sum rule (EWSR)], $E1$ (27%* EWSR), $E2$ (72% EWSR), and $E3$(31% EWSR) strength in ^{24}Mg were identified with 1–2-MeV resolution. Recently we reported a study of ^{24}Mg (and ^{28}Si) with inelastic scattering of 240-MeV ^{6}Li ions aimed at ascertaining the suitability of a ^{6}Li target for inverse reaction studies of the GMR [4]. We report here results from analyses of (new) data taken with 240-MeV α scattering using a detector system that measured both in- and out-of-plane angles [5]. In the experiments described in Ref. [3], only the in-plane angle was measured and the smallest effective angle was $1.1°$, whereas in the measurements reported here, the smallest effective angle is $0.4°$, which is potentially an important improvement, particularly for the monopole resonance for which the peak of the cross section occurs at $0°$. We also report a reanalysis of the data reported in Ref. [3], exploring a wide range of continuum choices to ascertain realistic errors resulting from the choice of continuum, while also analyzing the data with narrow energy bins in this light nucleus where there is considerable structure in the giant resonances. The results of this reanalysis were reported in Ref. [4].

Experimental details for the measurements are described in Ref. [5] and are summarized briefly in the following discussion. A beam of 240-MeV α particles from the Texas A&M K500 superconducting cyclotron bombarded a self-supporting ^{24}Mg foil 3.74 mg/cm^2 thick enriched to 99.96% in ^{24}Mg located in the target chamber of the multipole-dipole-multipole spectrometer. The acceptance of the spectrometer was $5°$ horizontally and $6°$ vertically, and ray tracing was used to reconstruct the scattering angle. Four resistive wire

detectors were used to measure the horizontal position in the focal plane and the in-plane scattering angle. Two drift chambers, placed before and after the resistive wire detector, were used to measure vertical position and the out-of-plane scattering angle. Data were taken at spectrometer angles of $0°$, $4.0°$, and $6.0°$, covering from $0°$ to $8.4°$ in the center of mass. Sample spectra obtained with this system are shown in Fig. 1. The data taken with the spectrometer at $0°$ were binned into six angles corresponding to $0.47°$, $1.11°$, $1.78°$, $2.46°$, $3.10°$, and $3.70°$, providing overlap with the data taken with the spectrometer at $4°$, which extended down to $3.1°$. The data taken at $4°$ and $6°$ were binned into 10 angles, each corresponding to $\Delta\theta \sim 0.4°$. In the scattering plane, a position resolution of approximately 0.9 mm and a scattering angle resolution of about $0.09°$ were obtained. The out-of-plane scattering angle resolution is ρ dependent because of the properties of the spectrometer and was approximately $0.3°$ in the giant resonance region improving to better than $0.1°$ at $E_x \sim 50$ MeV.

As there are processes in addition to multipole excitation prevalent at higher excitation that are not well understood, these processes are usually treated as a continuum and subtracted from the data, with the assumption that the remaining events result from multipole excitation. In the analysis of the new data and reanalysis of the data reported in Ref. [3], we chose several continua and then for each continuum choice did a complete multipole analysis. Examples of low and high continuum choices are shown superimposed on the spectra in Fig. 1.

After subtracting the continuum, the multipole components of the giant resonance peak were obtained by dividing the peak into multiple regions (bins) by excitation energy and then comparing the angular distributions obtained for each of these bins with distorted-wave Born approximation (DWBA) calculations to obtain the multipole components. The uncertainty from the multipole fits was determined for each multipole by incrementing (or decrementing) that strength and then adjusting the strengths of the other multipoles to minimize total χ^2. This continued until the new (χ^2 was 1 unit larger than the total χ^2 obtained for the best fit). Samples of the angular distributions obtained in this work are shown in Fig. 2. The final strength distributions were then obtained by averaging those distributions obtained with "reasonable" assumptions about the continuum, and the error bars on the multipole distributions represent the summation in quadrature of the errors for the individual

---

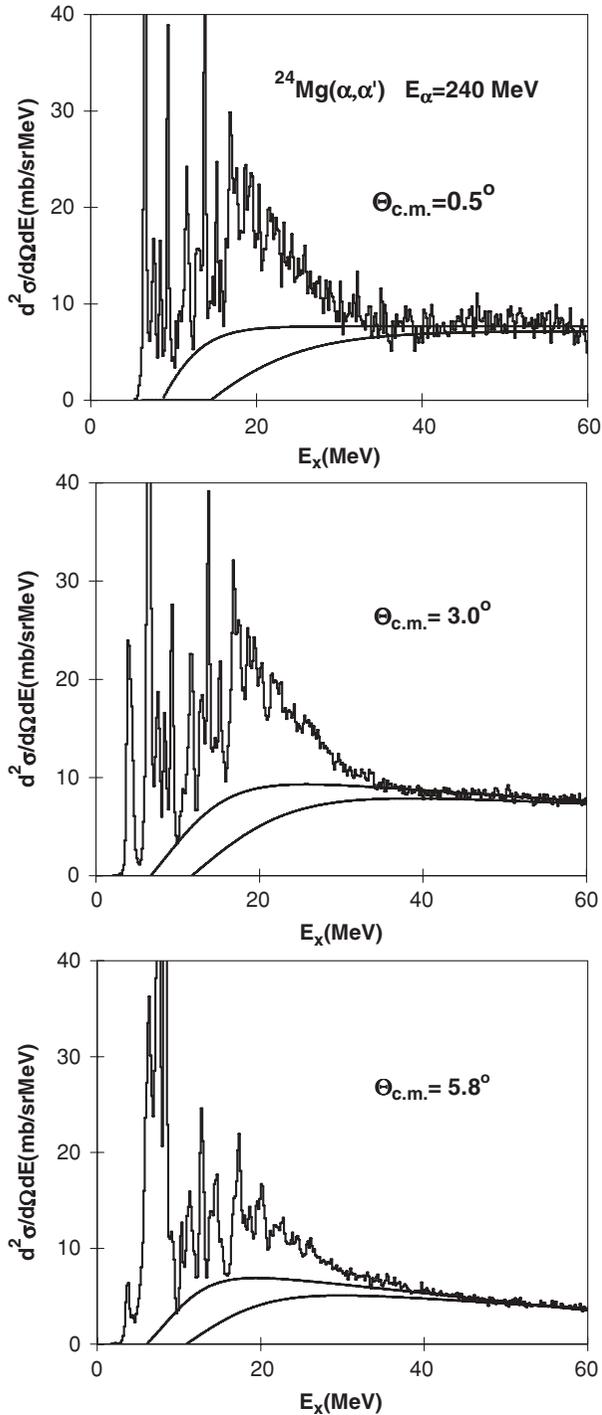*Present Address: Washington University, St. Louis, Missouri 63130, USA.

FIG. 1. Inelastic α spectra obtained for average cm angles of $0.5°$, $3.0°$, and $5.8°$. The lines show two continua used for the analysis.
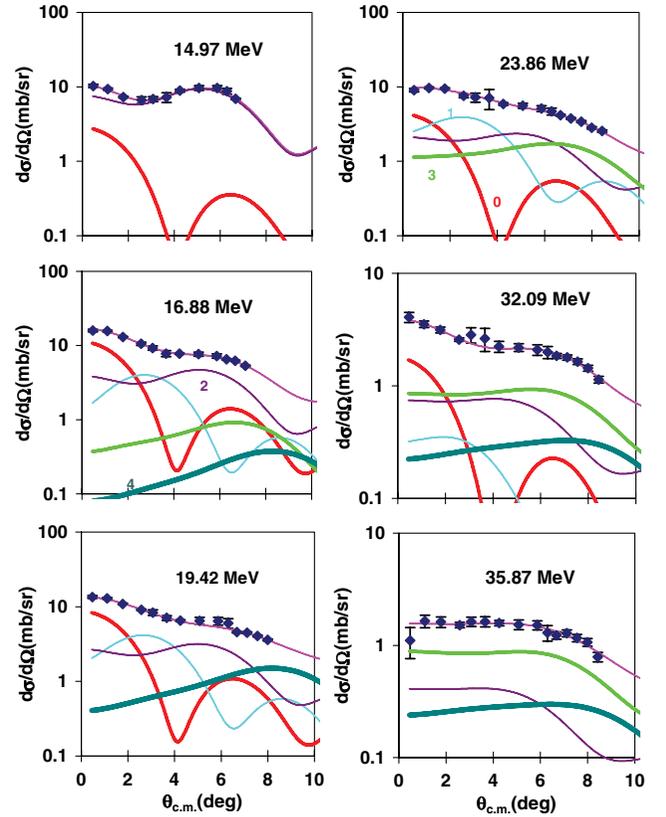

FIG. 2. (Color online) Angular distributions obtained for inelastic α scattering for six excitation energies of the giant resonance peak). The energy bins are approximately 600 keV wide. The line through the data shows the fits. Contributions of each multipole are shown, and the L transfer is indicated.

analysis and the standard deviation (for each energy bin) for all the analyses.

The DWBA calculations were described in Ref. [3], and the same density-dependent folding potentials were used for the calculations in this work. Fits to the angular distributions were carried out with a sum of isoscalar 0^+, 1^-, 2^+, 3^-, and 4^+ strengths. The isovector giant dipole resonance (IVGDR) contributions are small, but they were calculated from the

known distribution [6] and held fixed in the fits. Fits obtained, along with the individual components of the fits, are shown superimposed on the data in Fig. 2.

The (isoscalar) multipole distributions obtained from analysis of the data taken, including measuring the out-of-plane angle ("with vertical") and those obtained from a reanalysis of the data reported in Ref. [3] ("no vertical") are shown in Fig. 3 along with the distributions reported in Ref. [3]. The monopole distributions are in fairly good agreement, with the most recent data showing a little more 0^+ strength particularly in the narrower peaks. The peak at $E_x \sim 32$ MeV in the new data ("with vertical") appears considerably stronger than in the older data; however, only one of the two points disagree with outside errors. The isoscalar giant dipole resonance (ISGDR) and giant quadrupole resonance (GQR) distributions obtained in the recent analysis of the Ref. [3] data show substantially more strength than in the original analysis, primarily because of the continuum choices. The giant octupole resonance (GOR) distributions are roughly in agreement above $E_x \sim 15$ MeV (except for the energy resolution). A strong $L = 3$ peak shown in the analysis of Ref. [3] at $E_x \sim 9$ MeV is almost absent in the reanalysis, but there is strength in the reanalysis at $E_x \sim 11$ MeV and $E_x \sim 16$ MeV that does not show up in the original analysis reported in Ref. [3].

The strengths, centroids, and rms widths for the different multipole distributions obtained from the two analyses

TABLE I. Moments of isoscalar $E0$, $E1$, $E2$, and $E3$ distributions in ^{24}Mg.

	GMR			
	m_1 (% EWSR)	m_1/m_0 (MeV)	rms Width (MeV)	$(m_3/m_1)^{1/2}$ (MeV)
^{6}Li [4]	106^{+34}_{-24}	$21.35^{+0.37}_{-0.26}$	$4.98^{+0.68}_{-0.32}$	
Ref. [3]	72 ± 10	21.0 ± 0.6	7.3 ± 1.2	
Reanalyzed Ref. [3]	73 ± 8	21.3 ± 0.4	$6.5^{+0.6}_{-0.3}$	$24.0^{+0.7}_{-0.3}$
With vertical	82 ± 9	$21.9^{+0.3}_{-0.2}$	$6.5^{+0.5}_{-0.3}$	$24.7^{+0.5}_{-0.3}$
Pèru *et al.* [9]	94	20.57		
	ISGDR			
	m_1 (% EWSR)	m_1/m_0 (MeV)	rms Width (MeV)	
^{6}Li [4]	84^{+24}_{-21}	$26.56^{+0.29}_{-0.26}$	$6.42^{+0.29}_{-0.27}$	
Ref. [3]	27^{+9}_{-5}	18.8 ± 1.7	6.7 ± 1.0	
Reanalyzed Ref. [3]	50 ± 8	21.5 ± 0.4	$6.5^{+0.6}_{-0.4}$	
With vertical	65 ± 7	22.7 ± 0.4	6.2 ± 0.6	
	GQR			
	m_1 (% EWSR)	m_1/m_0 (MeV)	rms Width (MeV)	
^{6}Li [4]	76^{+14}_{-12}	$20.23^{+0.25}_{-0.20}$	$6.29^{+0.34}_{-0.25}$	
Ref. [3]	72 ± 10	16.9 ± 0.6	3.4 ± 0.6	
Reanalyzed Ref. [3]	88 ± 10	19.4 ± 0.3	7.2 ± 0.3	
With vertical	89 ± 10	19.9 ± 0.2	7.3 ± 0.3	
Pèru *et al.* [9]	87	19.84		
	GOR			
	m_1 (% EWSR)	m_1/m_0 (MeV)	rms Width (MeV)	
^{6}Li [4]	3^{+4}_{-1}	$18.54^{+1.40}_{-0.38}$	$5.85^{+0.28}_{-0.19}$	
Ref. [3]	31^{+9}_{-6}	25.2 ± 1.0	4.5 ± 1.2	
Reanalyzed Ref. [3]	29 ± 4	20.2 ± 0.3	8.5 ± 0.3	
With vertical	42 ± 5	$25.4^{+0.5}_{-0.3}$	8.3 ± 0.6	

reported here are compared with those from Ref. [3] and those obtained with inelastic ^{6}Li [4] scattering in Table I. The centroids and strengths obtained for the GMR in all the analyses of α scattering and ^{6}Li scattering are in agreement within errors, whereas the width obtained from the ^{6}Li data is somewhat lower than that obtained from α scattering. There are substantial differences between the different analyses and measurements for the other multipoles, however. For the ISGDR, considerably more strength is seen in the ^{6}Li scattering than in either analysis of the "no vertical" α data, although within errors, the strength seen in the "with vertical" α data and ^{6}Li agree, but the centroids differ by 3.8 MeV as strong ISGDR excitation between $E_x \sim 30$ and 35 MeV indicated from the ^{6}Li data is not seen in the α data. The original analysis from Ref. [3] of the "no vertical" α data shows about 60% of the strength and a centroid 2.7 MeV lower than the recent analysis of the same data. This difference is from differing continuum choices, emphasizing the sensitivity of the extracted ISGDR strength to the continuum choice. The GQR strengths obtained from our analysis of the two α data sets are in excellent agreement, whereas the centroids and widths of the GQR strength obtained from the ^{6}Li data are slightly different,

although the distributions appear quite similar [4]. The analysis reported in Ref. [3] used a higher continuum, which cut off some of the strength above $E_x \sim 25$ MeV as shown in Fig. 3, resulting in less strength and a considerably lower centroid. The results from the four analyses listed in Table I show very different parameters for the octupole resonance. Almost no strength (3%) was observed in the ^{6}Li scattering, whereas 42% of the sum rule was seen in the analysis of the data where the out-of-plane angle was measured.

There is a pattern to the results for the different multipoles. The $L = 0$ transfer has the most distinctive angular distribution because it peaks strongly at $0°$ and has a peak $\sim$60 times its minimum cross section over the angle range measured. Here the different measurements and analyses shown in Table I agree fairly well. The $L = 2$ and $L = 3$ transfers have smaller cross sections, and the distributions are somewhat flat over the angle range measured with about a factor of 3–4 difference between the maxima and the minima in the lower excitation region, making these distributions less distinctive. Also, all distributions become flatter at higher excitation, particularly affecting the high-energy octupole resonance [7] located around $3\hbar\omega$ and resulting in the large variation in $L = 3$ strength seen
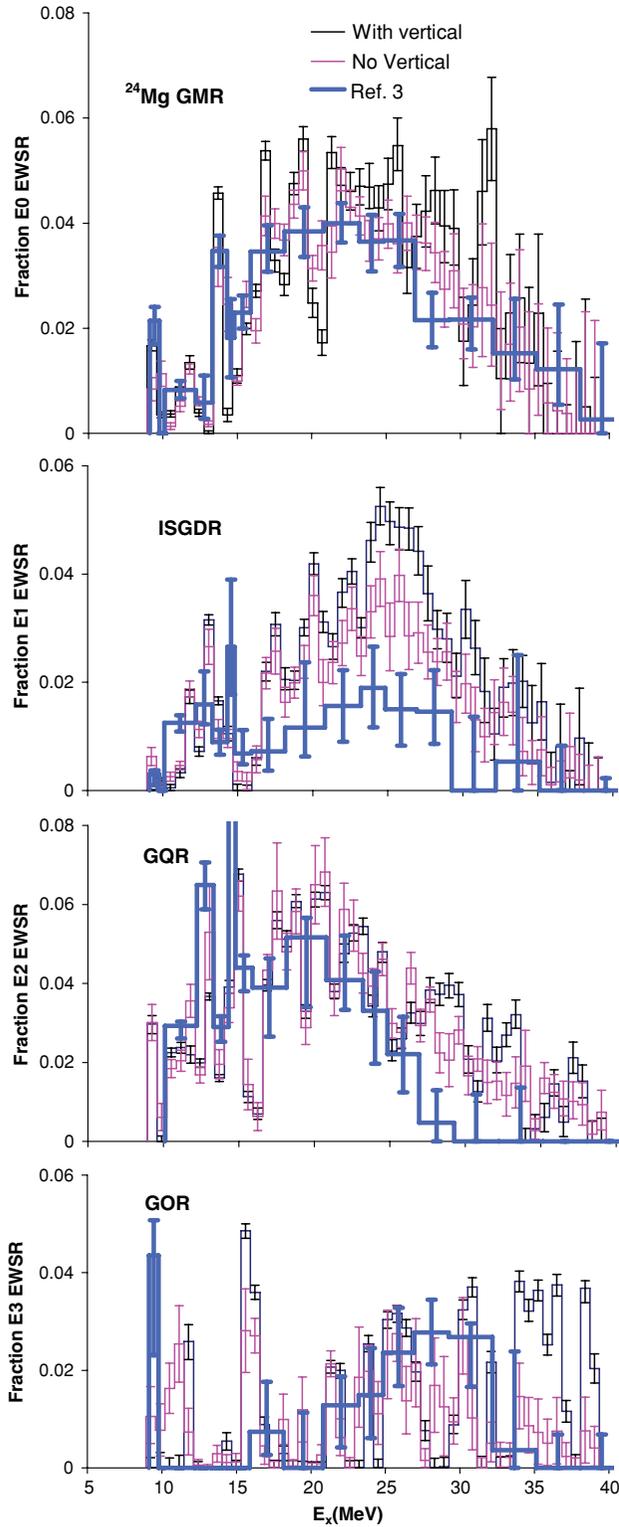
FIG. 3. (Color online) The multipole strength distributions obtained are shown. The black histogram shows those obtained by analyzing the data for which the out-of-plane angle was measured. The gray histogram shows those obtained in the reanalysis of the data reported in Ref. [3] (in-plane only), and the wide gray histograms show the distributions reported in Ref. [3]. Error bars represent the uncertainty from the fitting of the angular distributions as described in the text and do not include systematic errors.

in the different analyses. The ISGDR distribution has a peak ~20 times its minimum cross section at lower excitation, but in 240-MeV α scattering in many nuclei [8] including ^{24}Mg [3], the continuum angular distribution is very similar to that of the ISGDR, making the extracted strength very sensitive to continuum choices. Much of the ISGDR strength also lies at higher excitation where the angular distributions are less distinctive.

Pèru, Goutte, and Berger [9] have calculated GMR, ISGDR, and GQR distributions in ^{24}Mg and ^{28}Si using the quasi-particle random phase approximation based on Hartree-Fock-Bogolyubov states calculated with the Gogny D1S effective force. These are shown compared with multipole distributions obtained with ^{6}Li scattering and α scattering in Figs. 19 and 20 of Ref. [4]. The agreements with the GMR distributions are fairly good, but there are substantial differences for the ISDGR and GQR distributions. They give centroids and strengths for the GQR and GMR distributions, and these are compared with our results for ^{24}Mg in Table I. The GMR centroid they obtain is a little lower than the experimental numbers (but within the errors for the results from the Ref. [3] data), whereas they report somewhat more strength than seen in the α data but within the (relatively large) errors in agreement with the strength obtained in the ^{6}Li data. The GQR strength and centroids are in agreement with the analysis of the α data reported in this work and only slightly outside the errors for the ^{6}Li results. The Gogny D1S interaction used by Pèru, Gouette, and Berger [9] results in a $K_{nm} = 228$ MeV [10]. In the hydrodynamic model [11], $E_{GMR} = (\hbar^2 K_A/m^* \langle r^2 \rangle)^{1/2}$, where K_A is the compressibility of nucleus A. We have estimated the K_{nm} values implied by the ^{24}Mg GMR energy obtained in this experiment and the ^{28}Si GMR energy reported in Ref. [12] by comparing them with the
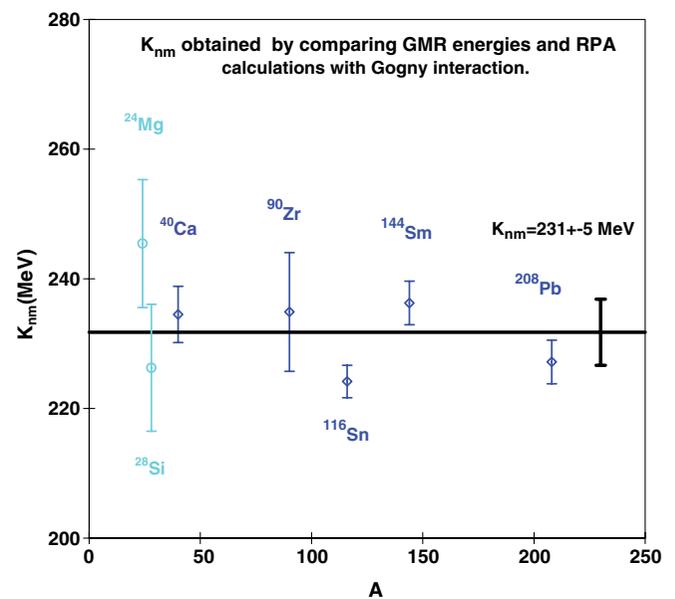

FIG. 4. (Color online) K_{nm} obtained by comparing GMR energies in ^{24}Mg and ^{28}Si with the calculations of Ref. [9] as described in the text, and for ^{40}Ca, ^{90}Zr, ^{116}Sn, ^{144}Sm, and ^{208}Pb as reported in Ref. [13]. The average value reported in Ref. [13] is also shown along with its uncertainty.

energies obtained by Pèru, Gouette, and Berger [9], assuming that K_{nm} scales with K_A and hence that $\Delta K_{nm}/K_{nm} = 2\Delta E_{GMR}/E_{GMR}$. These values with errors corresponding to the uncertainties in the experimental energies are plotted in Fig. 4 along with the values reported in Ref. [13], where the GMR energies in ^{208}Pb, ^{144}Sm, ^{116}Sn, ^{90}Zr, and ^{40}Ca were compared with Hartree-Fock random-phase approximation calculations using Gogny interactions by Blaizot *et al.* [14] to obtain K_{nm}. Even for these light, deformed nuclei, the K_{nm} values obtained are in reasonable agreement with those from the heavier nuclei and with the average value reported in that work.

[1] H. J. Lu, S. Brandenburg, R. De Leo, M. N. Harakeh, T. D. Poelhekken, and A. van der Woude, Phys. Rev. C **33**, 1116 (1986).

[2] H. Dennert, E. Aschenauer, W. Eyrich, A. Lehmann, M. Moosburger, N. Scholz, H. Wirth, H. J. Gils, H. Rebel, and S. Zagromski, Phys. Rev. C **52**, 3195 (1995).

[3] D. H. Youngblood, Y.-W. Lui, and H. L. Clark, Phys. Rev. C **60**, 014304 (1999).

[4] X. Chen, Y.-W. Lui, H. L. Clark, Y. Tokimoto, and D. H. Youngblood, Phys. Rev. C **80**, 014312 (2009).

[5] D. H. Youngblood, Y.-W. Lui, B. John, Y. Tokimoto, H. L. Clark, and X. Chen, Phys. Rev. C **69**, 054312 (2004).

[6] S. S. Dietrich and B. L. Berman, At. Data Nucl. Data Tables **38**, 199 (1988).

[7] M. Harakeh and A. van der Woude, *Giant Resonances* (Oxford University Press, New York, 2001), Chap. 4, p. 156.

[8] D. H. Youngblood, Y.-W. Lui, H. L. Clark, B. John, Y. Tokimoto, and X. Chen, Phys. Rev. C **69**, 034315 (2004).

[9] S. Pèru, H. Goutte, and J. F. Berger, Nucl. Phys. **A788**, 44c (2007).

[10] J. Decharge and D. Gogny, Phys. Rev. C **21**, 1568 (1980).

[11] J. Treiner, H. Krivine, O. Bohigas, and J. Martorell, Nucl. Phys. **A371**, 253 (1981).

[12] D. H. Youngblood, Y.-W. Lui, and H. L. Clark, Phys. Rev. C **76**, 027304 (2007).

[13] D. H. Youngblood, H. L. Clark, and Y.-W. Lui, Phys. Rev. Lett. **82**, 691 (1999).

[14] J. P. Blaizot *et al.*, Nucl. Phys. **A591**, 435 (1995).